Available online at www.sciencedirect.com
SCIENCE DIRECT®
Acta Materialia 53 (2005) 2643–2652
Acta MATERIALIA
www.actamat-journals.com

First-principles study of constitutional point defects in B2 NiAl using special quasirandom structures

Chao Jiang [a,b,*], Long-Qing Chen [a], Zi-Kui Liu [a]

[a] Department of Materials Science and Engineering, The Pennsylvania State University, University Park, PA 16802, USA
[b] Department of Materials Science and Engineering, Iowa State University, Ames, IA 50011, USA

Received 7 January 2005; received in revised form 3 February 2005; accepted 11 February 2005
Available online 2 April 2005

Abstract

We developed special quasirandom structures (SQSs) for substitutionally random pseudobinary $A_{1-x}B_xC$ B2 alloys at compositions $x = 0.25$ and 0.5. The structures mimic the local pair and multisite correlation functions of the corresponding random simple-cubic alloy. Our SQSs were applied to study non-stoichiometric B2 NiAl alloys containing high concentrations of constitutional point defects. Direct first-principles calculations on the SQSs provide formation enthalpies, equilibrium lattice parameters and elastic constants of non-stoichiometric B2 NiAl alloys in satisfactory agreement with existing experimental data in the literature. Our calculations unambiguously show that Ni vacancies and Ni antisites are the stable constitutional point defects in Al-rich and Ni-rich B2 NiAl, respectively, up to large deviations from stoichiometry. Our SQS calculations also confirmed the experimentally observed structural instability of B2 NiAl at high Ni concentrations. Finally, we demonstrated that our SQSs can even give formation enthalpies of isolated defects in good agreement with 54-atom supercell calculations.

Keywords: Nickel aluminides; Point defects; First-principles; Special quasirandom structures

1. Introduction

The intermetallic compound β-NiAl is routinely employed in high-temperature applications due to its high melting temperature, good oxidation resistance, high thermal conductivity and low density [1]. It is stable over a wide composition range [2] with an ordered B2 (CsCl-type) structure, which consists of two interpenetrating simple-cubic sublattices with each sublattice having the same number of lattice sites. In its perfectly ordered state at stoichiometric composition, one sublattice is entirely occupied by Al and the other entirely by Ni atoms. Deviations from ideal stoichiometry are accommodated by the formation of constitutional (structural) point defects (e.g., vacancies and antisites). In Al-rich and Ni-rich B2 NiAl alloys, those constitutional point defects are Ni vacancies and Ni antisites, respectively [3]. The existence of those point defects is of great technological importance as they strongly affect such important properties of B2 alloys as mechanical properties and diffusion mechanisms [4–6].

Extensive first-principles studies of point defects in B2 NiAl have been performed in the literature [7–12]. Recently, the site preference of Pt in B2 NiAl has also been studied using first-principles calculations by Jiang et al. [13]. In those studies, large supercells containing N sites and only one point defect were employed to obtain properties of isolated point defects in stoichiometric B2 NiAl and properties at non-dilute defect concentrations have to be obtained through linear extrapolation from the dilute limit, e.g., the Wagner–Schottky model (a gas of non-interacting point defects on well-defined

* Corresponding author. Tel.: +1 515 294 0739; fax: +1 515 294 5444.
E-mail address: chaoisu@iastate.edu (C. Jiang).

1359-6454/$30.00
doi:10.1016/j.actamat.2005.02.026

sublattices) [14]. In contrast, the purpose of the present study was to directly obtain properties of non-stoichiometric B2 NiAl containing high concentrations of defects by means of first-principles calculations. However, the situation now becomes complicated due to the compositional disorder caused by the significant number of point defects.

The brute force way to treat non-stoichiometric compounds with concentrated point defects would be to construct a large supercell and randomly distribute the point defects on the host lattice. This would necessarily require very large supercells to adequately mimic the statistics of random alloys. Since first-principles calculations based on density functional theory (DFT) [15] are computationally constrained by the number of atoms that one can treat, such an approach could be computationally prohibitive. Therefore, in this study, we adopted the special quasirandom structure (SQS) approach proposed by Zunger et al. [16,17]. SQSs are specially designed small-unit-cell periodic structures with only a few (8–32) atoms per unit cell, which closely mimic the most relevant local pair and multisite correlation functions of the random substitutional alloys. Due to the small sizes of the SQSs, essentially any DFT method can be employed, including full-potential methods capable of accurately capturing the effects of atomic relaxations.

Admittedly, the SQS approach is inapplicable for studying physical properties that depend on all correlation functions, not just the first few nearest ones. Fortunately, there are many important alloy properties that are local environmentally dependent. For example, the SQS approach has been applied extensively to study the formation enthalpies, bond length distributions, density of states, band gaps and optical properties in semiconductor alloys [16–18]. They have been applied to investigate the local lattice relaxations in size-mismatched transition metal alloys [19–22] and to predict the formation enthalpies of Al-based fcc alloys [23]. Recently, SQSs for binary body-centered cubic (bcc) alloys have also been developed to study their formation enthalpies, equilibrium lattice parameters, magnetic moments and nearest-neighbor bond lengths [24].

In this paper, we further developed SQSs for random pseudobinary $A_{1-x}B_xC$ B2 alloys. Here A and B atoms are randomly distributed on one B2 sublattice with the second sublattice completely occupied by C atoms. The substitutional alloy problem is thus simple-cubic-based. It is straightforward to apply our SQSs to model non-stoichiometric B2 NiAl compounds containing different types of constitutional point defects by treating them as corresponding pseudobinary B2 alloys. We treat B2 NiAl containing Ni vacancies, Al vacancies, Ni antisites and Al antisites as $Ni_{1-x}Va_xAl$, $Al_{1-x}Va_xNi$, $Al_{1-x}Ni_xNi$ and $Ni_{1-x}Al_xAl$ pseudobinary B2 alloys, respectively. Here Va denotes vacancy. It is noted that the present SQSs only consider the temperature-independent constitutional point defects. At finite temperatures, thermal defects will also be activated in addition to the constitutional ones by entropy. As single point defects in ordered alloys alone are not composition conserving, those thermal defects appear in balanced combinations in order to maintain the overall composition of the alloy. For example, the dominant thermal defects in B2 NiAl are triple-defects, i.e., simultaneous generation of two Ni vacancies and one Ni antisite [1]. Nevertheless, since B2 NiAl is strongly ordered (its A2–B2 order–disorder transition temperature is well above its melting temperature [25]), the concentrations of those thermal defects are orders of magnitude smaller than those of the constitutional ones even at high temperatures [26]. As the result, it is still a good approximation to represent non-stoichiometric B2 NiAl at finite temperatures using the present SQSs.

In the subsequent sections, we will first give a detailed description of the SQS approach. The first-principles methods we adopted will then be described. Finally, we demonstrate the usefulness of our SQSs by applying them to predict the formation enthalpies, equilibrium lattice parameters and elastic constants of non-stoichiometric B2 NiAl; the results are compared with the existing experimental data in the literature.

2. Generation of special quasirandom structures

For a binary $A_{1-x}B_x$ substitutional alloy, many properties such as energy are dependent on the configuration, or the substitutional arrangement of A and B atoms on the lattice. The configuration dependence of properties can be efficiently characterized by a "lattice algebra" [16,17,19,20]: Pseudo-spin variables are assigned to each site, $S_i = -1$ (+1) if an A (B) atom sits at site i. We further define geometric figures f as symmetry-related groupings of lattice sites, e.g., single site, nearest-neighbor pair, three-body figures, etc. Those figures $f = (k,m)$ can have k vertices and span a maximum distance of m ($m = 1, 2, 3\ldots$ are the first-, second- and third-nearest neighbors, etc.). By taking the product of the spin variables over all sites of a figure, and averaging over all symmetry-equivalent figures of the lattice, we obtain the correlation functions $\bar{\Pi}_{k,m}$ [16,17]. For the perfectly random $A_{1-x}B_x$ alloy, there is no correlation in the occupation between various sites, and therefore the pair and multisite correlation function $\bar{\Pi}_{k,m}$ can be simply written as $\langle\bar{\Pi}_{k,m}\rangle_R = (2x-1)^k$, i.e., the product of the lattice-averaged site variable, which is related to the composition by $\langle S_i\rangle = 2x - 1$.

The SQS approach in essentially finding the small-unit-cell ordered structures that possess $(\bar{\Pi}_{k,m})_{SQS} \cong \langle\bar{\Pi}_{k,m}\rangle_R$ for as many figures as possible. Admittedly, describing random alloys by small unit-cell periodically

repeated structures will surely introduce erroneous correlations beyond a certain distance. However, since interactions between widely separated atoms are expected to be weaker than interactions between nearer ones, we can construct SQSs that exactly reproduce the correlation functions of a random alloy between the first few nearest neighbors, deferring periodicity errors to more distant neighbors.

In the present study, we have generated various SQS-N structures for the random pseudobinary $A_{1-x}B_xC$ B2 alloys (with $N = 4$ and 16 simple-cubic sites per unit cell, or a total of $2N$ atoms per unit cell including the common C sublattice) at compositions where $x = 0.5$ and 0.25. For each composition x, our procedure can be described as follows: (1) using the *gensqs* code in the alloy-theoretic automated toolkit (ATAT) [27], we exhaustively generate all structures based on the simple-cubic lattice with N simple-cubic sites per unit cell and composition x; (2) we then construct the pair and multisite correlation functions $\bar{\Pi}_{k,m}$ for each structure; (3) finally, we search for the structure(s) that best match the correlation functions of random alloys over a specified set of pair and multisite figures. Our search criterion requires that the pair correlation functions of the structure be identical to those of the random alloy up to the third-nearest neighbor (in the present notation, the simple cubic first-, second- and third-nearest neighbors are equivalent to the second-, third- and fifth-nearest neighbors in the B2 structure, respectively). For $x = 0.5$, we find one such SQS already for $N = 4$. For $x = 0.25$, however, we found that we need a SQS-16 structure to satisfy our criterion. To further investigate the convergence of the SQSs with respect to the size of the unit cell, we also generate one SQS-16 structure for $x = 0.5$ whose pair correlation functions are identical to those of the random alloy up to the 14th-nearest neighbor.

The lattice vectors and atomic positions of the obtained SQS-N structures in their ideal, unrelaxed forms are given in Table 1, all in Cartesian coordinates. The positions of all the atoms on the common C sublattice are also included. The definitions of the multisite figures considered here are given in Table 2. In Table 3, the pair and multisite correlation functions of the SQS-N structures presented in Table 1 are compared with those of the corresponding random simple-cubic alloys. The SQS-N structures for $x = 0.75$ can be simply obtained by switching the A and B atoms in SQS-N for $x = 0.25$.

Unless specified, we use SQS-4 and SQS-16 to represent the random $A_{1-x}B_xC$ B2 alloy at composition

Table 1
Structural descriptions of the SQS-N structures

	$A_{0.5}B_{0.5}C$	$A_{0.75}B_{0.25}C$
SQS-16	Lattice vectors $\vec{a}_1 = (1.0, 2.0, 1.0)$, $\vec{a}_2 = (1.0, 0.0, -1.0)$ $\vec{a}_3 = (-3.0, 2.0, -3.0)$ Atomic positions A – (−1.5, 2.5, −2.5), A – (−1.5, 1.5, −2.5) A – (0.5, 1.5, −1.5), A – (−0.5, 1.5, −2.5) A – (−1.5, 2.5, −3.5), A – (−1.5, 3.5, −2.5) A – (0.5, 0.5, −1.5), A – (0.5, 0.5, −0.5) B – (−0.5, 1.5, −1.5), B – (−0.5, 2.5, −2.5) B – (−0.5, 2.5, −1.5), B – (−0.5, 3.5, −2.5) B – (0.5, 1.5, −0.5), B – (0.5, 2.5, −1.5) B – (0.5, 2.5, −0.5), B – (1.5, 1.5, −0.5) C – (−2.0, 2.0, −3.0), C – (0.0, 3.0, −1.0) C – (−1.0, 2.0, −3.0), C – (−1.0, 2.0, −2.0) C – (−1.0, 3.0, −3.0), C – (−1.0, 3.0, −2.0) C – (0.0, 1.0, −2.0), C – (0.0, 1.0, −1.0) C – (0.0, 2.0, −2.0), C – (0.0, 2.0, −1.0) C – (0.0, 3.0, −2.0), C – (−1.0, 4.0, −3.0) C – (1.0, 1.0, −1.0), C – (1.0, 2.0, −1.0) C – (1.0, 2.0, 0.0), C – (−2.0, 3.0, −3.0)	Lattice vectors $\vec{a}_1 = (3.0, 1.0, 1.0)$, $\vec{a}_2 = (-1.0, -3.0, 1.0)$ $\vec{a}_3 = (-1.0, 1.0, -3.0)$ Atomic positions A – (1.5, −1.5, 0.5), A – (2.5, 0.5, 0.5) A – (0.5, −0.5, −0.5), A – (1.5, 0.5, −0.5) A – (−0.5, 0.5, −2.5), A – (1.5, −0.5, 0.5) A – (1.5, −0.5, −0.5), A – (−0.5, −1.5, −1.5) A – (0.5, −0.5, −1.5), A – (−0.5, −0.5, −1.5) A – (0.5, 0.5, −1.5), A – (0.5, −1.5, −0.5) B – (−0.5, −1.5, −0.5), B – (−0.5, −2.5, 0.5) B – (0.5, −1.5, 0.5), B – (1.5, 0.5, −1.5) C – (2.0, 1.0, −1.0), C – (−1.0, −2.0, −1.0) C – (2.0, 0.0, 0.0), C – (0.0, −1.0, −1.0) C – (0.0, 0.0, −1.0), C – (1.0, 0.0, −1.0) C – (0.0, −2.0, 0.0), C – (2.0, −1.0, 1.0) C – (0.0, −1.0, 0.0), C – (1.0, −1.0, 0.0) C – (1.0, −1.0, −1.0), C – (1.0, 0.0, 0.0) C – (1.0, −2.0, 1.0), C – (−1.0, −1.0, −2.0) C – (0.0, 0.0, −2.0), C – (1.0, 1.0, −2.0)
SQS-4	Lattice vectors $\vec{a}_1 = (2.0, 1.0, 1.0)$, $\vec{a}_2 = (1.0, 1.0, 2.0)$ $\vec{a}_3 = (1.0, 2.0, 1.0)$ Atomic positions A – (0.5, 0.5, 0.5), A – (3.5, 3.5, 3.5) B – (1.5, 1.5, 1.5), B – (2.5, 2.5, 2.5) C – (0.0, 0.0, 0.0), C – (1.0, 1.0, 1.0) C – (2.0, 2.0, 2.0), C – (3.0, 3.0, 3.0)	

Lattice vectors and atomic positions are given in Cartesian coordinates, in units of a, the B2 lattice parameter. Atomic positions are given for the ideal, unrelaxed B2 sites.

Table 2
Vertices of the multisite figures, given in units of a, the B2 lattice parameter

Type	Figure designation	Vertices			
Triplets	(3,2)	(0,0,0)	(0,0,1)	(0,1,1)	
Quadruplets	(4,2)	(0,0,0)	(1,1,0)	(1,0,1)	(0,1,1)

Table 3
Pair and multisite correlation functions of SQS-N structures

Figure	$x = 0.5$			$x = 0.25$	
	Random	SQS-16	SQS-4	Random	SQS-16
$\bar{\Pi}_{2,1}$ [3]	0	0	0	0.25	0.25
$\bar{\Pi}_{2,2}$ [6]	0	0	0	0.25	0.25
$\bar{\Pi}_{2,3}$ [4]	0	0	0	0.25	0.25
$\bar{\Pi}_{2,4}$ [3]	0	0	−1	0.25	0
$\bar{\Pi}_{2,5}$ [12]	0	0	0	0.25	0.25
$\bar{\Pi}_{2,6}$ [12]	0	0	0	0.25	0.25
$\bar{\Pi}_{2,7}$ [6]	0	0	1	0.25	0
$\bar{\Pi}_{3,2}$ [12]	0	0	0	−0.125	−0.125
$\bar{\Pi}_{4,2}$ [2]	0	0	−1	0.0625	0

The number in the square brackets next to $\bar{\Pi}_{k,m}$ gives the degeneracy factor of the corresponding figure.

$x = 0.5$ and 0.25, respectively. SQS-4 for $x = 0.5$ is a trigonal-type 8-atom supercell with space group $R\bar{3}m$ (space group No. 166 in the International Tables of Crystallography), and SQS-16 for $x = 0.25$ is a trigonal-type 32-atom supercell with space group $R3m$ (space group No. 160 in the International Tables of Crystallography)

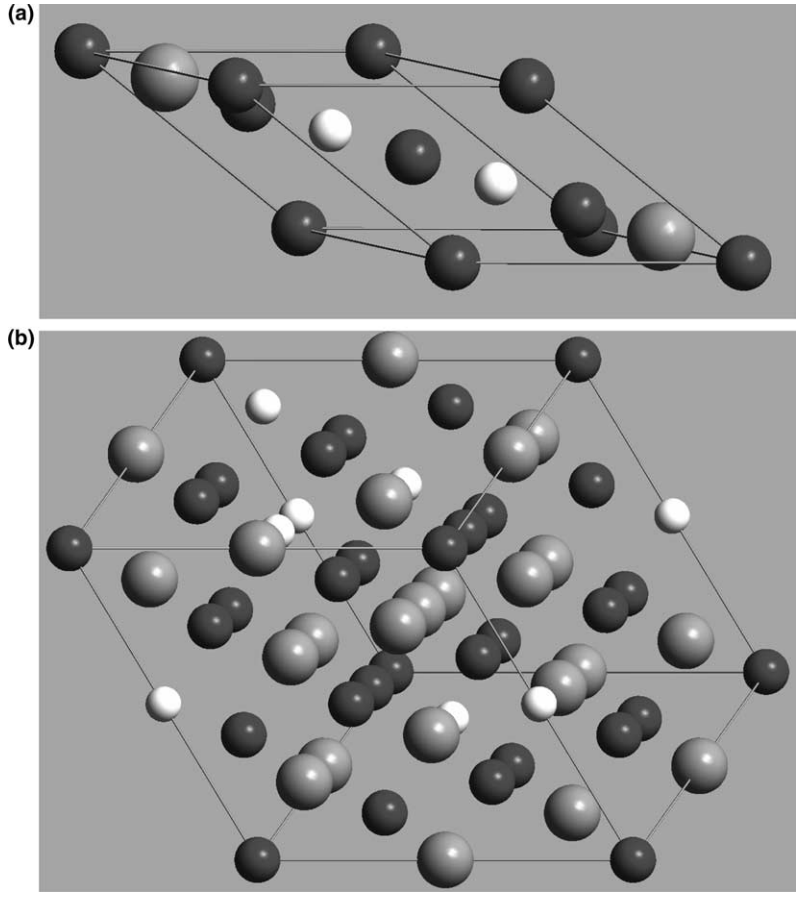

Fig. 1. Crystal structure of SQSs in their ideal, unrelaxed forms. Gray, white and dark spheres represent A, B and C atoms, respectively. (a) SQS-4 for $A_{0.5}B_{0.5}C$; (b) SQS-16 for $A_{0.75}B_{0.25}C$.

[28]. They are shown in Fig. 1 in their ideal, unrelaxed forms.

3. First-principles methodology

First-principles calculations were performed using the all-electron Blöchl's projector augmented wave (PAW) approach [29,30] within the generalized gradient approximation (GGA), as implemented in the highly efficient Vienna ab initio simulation package (VASP) [31,32]. For the GGA exchange-correlation functional, we employed the Perdew–Wang parameterization (PW91) [33,34]. The semi-core 3p electrons of Ni were explicitly treated as valence. The k-point meshes for Brillouin zone sampling were constructed using the Monkhorst–Pack scheme [35] and the total number of k-points times the total number of atoms per unit cell was at least 10,000 for all structures. A plane wave cutoff energy of 459.9 eV was used. Spin-polarized calculations were performed to account for the ferromagnetic nature of Ni though our calculations showed B2 NiAl as non-magnetic, in agreement with previous first-principles calculations [36].

3.1. Bulk modulus

We obtained elastic constants using the approach proposed by Mehl et al. [37]. To obtain the equilibrium volume and bulk modulus $B = (C_{11} + 2C_{12})/3$ of B2 NiAl, we fit the first-principles calculated total energies as a function of volume to a Birch–Murnaghan [38] equation of state:

$$E(V) = \sum_{n=0}^{2} a_n V^{-2n/3}, \tag{1}$$

where V is the volume of the unit cell. The equilibrium volume V_0 is obtained by letting $\frac{\partial E}{\partial V} = 0$, and the bulk modulus is calculated at the theoretical equilibrium volume V_0 as:

$$B(V) = V \left.\frac{\partial^2 E}{\partial V^2}\right|_{V=V_0}. \tag{2}$$

3.2. Shear modulus

To obtain the shear modulus $C' = (C_{11}C_{12})/2$, we applied a homogeneous volume-conserving orthorhombic strain to the underlying B2 lattice [37,39]:

$$\overleftrightarrow{\varepsilon} = \begin{pmatrix} \delta & 0 & 0 \\ 0 & -\delta & 0 \\ 0 & 0 & \delta^2/(1-\delta^2) \end{pmatrix} \tag{3}$$

and the distorted lattice vectors of the SQS unit cells were obtained via the following matrix multiplications [37]:

$$\overleftrightarrow{a}' = \overleftrightarrow{I} + \overleftrightarrow{\varepsilon} \cdot \overleftrightarrow{a}, \tag{4}$$

where $\overleftrightarrow{a}$ and $\overleftrightarrow{a}'$ are the matrix containing the old and new SQS lattice vectors, respectively. $\overleftrightarrow{I}$ is a 3×3 identity matrix. The distortion energy $\Delta E(\delta) = E(\delta) - E(0)$ (i.e., the total energy difference between the distorted and undistorted structures) can then be written as $\Delta E(\delta) = 2V_0 C'\delta^2 + O(\delta^4)$. To extract C', we fit the first-principles calculated distortion energies at $\delta = 0.005$, 0.01, 0.15 and 0.02 to the following function:

$$\Delta E(\delta) = \sum_{m=1}^{2} b_m \delta^{2m} \tag{5}$$

and we obtain $C' = b_1/2V_0$. It may be argued that, since our SQSs have lower-than-cubic symmetry, in principle they cannot be used to calculate the cubic elastic constants. However, both our SQS-4 structure for $x = 0.5$ and SQS-16 structure for $x = 0.25$ do strictly satisfy the condition $\Delta E(\delta) = \Delta E(-\delta)$ and also the calculated distortion energies are indeed independent of the choice of axis. Therefore, despite their seemingly low symmetries, they can still be used to give unique elastic shear modulus C'.

3.3. Formation enthalpies

In the present study, the unit cell volumes of all structures were fully relaxed. To further consider the effects of local atomic relaxations around point defects, we also fully relaxed all atoms from their ideal lattice sites into their equilibrium positions according to the quantum-mechanical Hellmann–Feynman forces using a quasi-Newton algorithm, maintaining the overall volume and shape of the unit cell. Due to limited computing resources, we did not consider such effects in our elastic constant calculations, i.e., we assume that all the atoms occupy their ideal lattice positions.

The formation enthalpy of a B2 NiAl alloy can be obtained from the following equation:

$$\Delta H(x_{\mathrm{Ni}}) = E(\mathrm{Ni}_{x_{\mathrm{Ni}}}\mathrm{Al}_{1-x_{\mathrm{Ni}}}) - (1 - x_{\mathrm{Ni}})E(\mathrm{Al}) - x_{\mathrm{Ni}}E(\mathrm{Ni}), \tag{6}$$

where E(Al), E(Ni) and $E(\mathrm{Ni}_x\mathrm{Al}_{1-x})$ are, respectively, the first-principles calculated total energies (per atom) of the constituent pure elements Al and Ni and the corresponding SQS, each relaxed to their equilibrium geometries. Here x_{Ni} is the molar composition of Ni in the alloy. In the present study, face-centered cubic (fcc) Al and ferromagnetic fcc Ni are used as reference states in Eq. (6).

4. Results and discussions

4.1. Formation enthalpies

In Fig. 2, the SQS calculated formation enthalpies of B2 NiAl containing each of the four types of

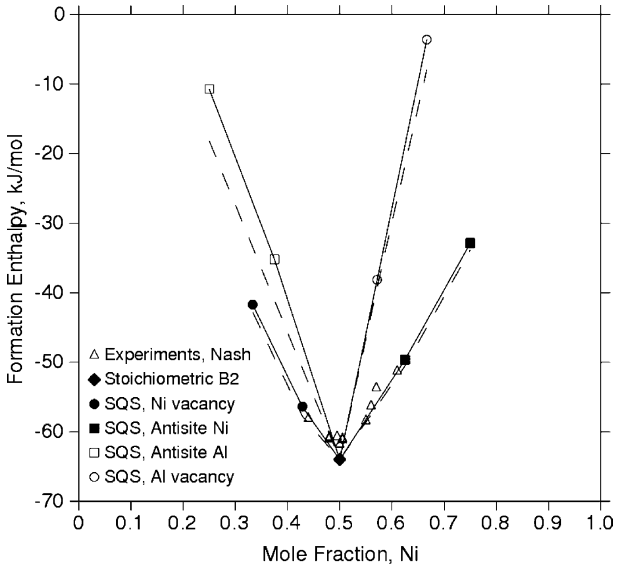

Fig. 2. Comparison between first-principles calculated and experimentally observed formation enthalpies of B2 NiAl as a function of composition. Experimental data are from Nash and Kleppa [40]. The solid and dashed lines correspond to unrelaxed (volume relaxations only) and fully relaxed (volume + local atomic relaxations) formation enthalpies, respectively.

constitutional point defects, Al antisite, Ni antisite, Al vacancy and Ni vacancy, are plotted as four branches, respectively. We consider a canonical ensemble containing a total one mole of Al and Ni atoms and the total number of lattice sites may vary when vacancies are present. Since deviation from stoichiometry can be accommodated by either constitutional antisites or constitutional vacancies, there are two branches on either side of the stoichiometric composition in Fig. 2, the branch with lower formation enthalpy corresponding to the stable one. Fig. 2 unambiguously shows that the stable constitutional point defects in Al-rich and Ni-rich B2 NiAl are Ni vacancies and Ni antisites, respectively. This conclusion is in accordance with Bradley and Taylor [3] and the previous first-principles studies [7–12]. For comparison, we also show in Fig. 2 the experimental measurements by Nash and Kleppa [40] using high temperature reaction calorimetry, in good agreement with our SQS calculations.

As has already been mentioned, non-stoichiometric B2 NiAl alloys were treated as corresponding random pseudobinary $(AC)_{1-x}(BC)_x$= $A_{1-x}B_xC$ B2 alloys in the present study. It is thus also interesting to calculate their mixing enthalpies (per formula unit) relative to the composition-weighted average of their end members rather than pure Al and Ni:

$$\Delta H_{\mathrm{mix}}(x) = E(\mathrm{A}_{1-x}\mathrm{B}_x\mathrm{C}) - (1-x)E(\mathrm{AC}) - xE(\mathrm{BC}), \tag{7}$$

where x is the site fraction of B (atoms or vacancies) on the simple-cubic sublattice and E is the total energy per $A_{1-x}B_xC$ formula unit. The total energies of the end members in Eq. (7) were obtained in the present study via first-principles calculations.

Fig. 3 shows the mixing enthalpies of Al-rich B2 NiAl containing Ni vacancies ($Ni_{1-x}Va_xAl$) and Ni-rich B2 NiAl containing Ni antisites ($Al_{1-x}Ni_xNi$) with respect to their respective end-members as a function of composition. As shown, the mixing enthalpies are all negative, thus indicating an ordering-tendency of the Ni vacancies as well as the Ni antisites on their respective sublattices. In fact, the formation of Ni_2Al_3 and Ni_5Al_3 phases in the Ni–Al system can be viewed as due to the ordering of constitutional Ni vacancies and Ni antisites on the Ni and Al sublattices, respectively, in such a way that no two defects are in nearest-neighbor position with each other [7].

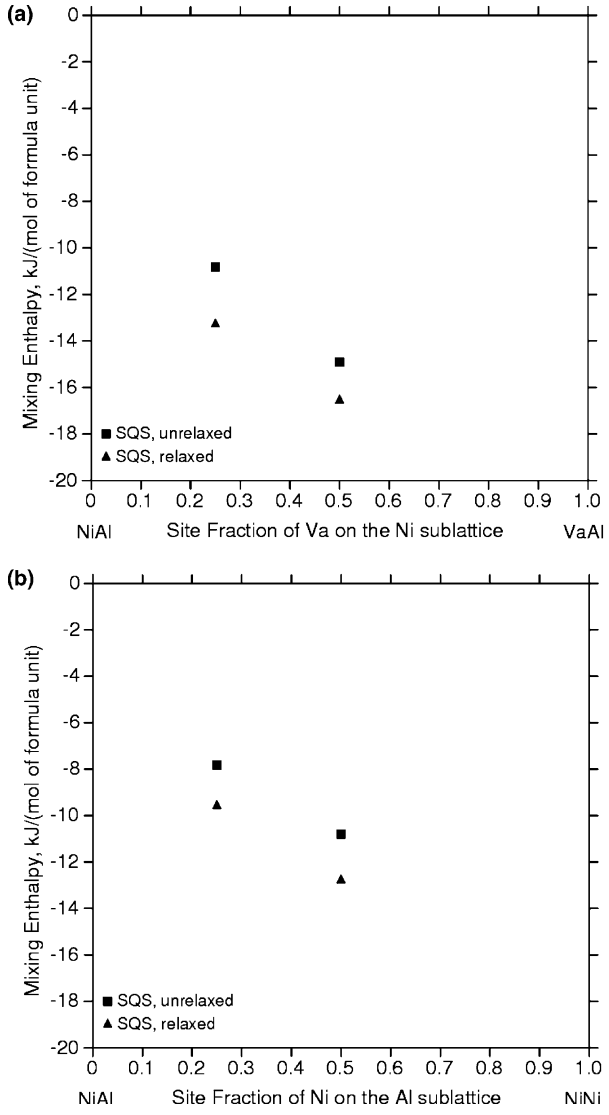

Fig. 3. First-principles calculated mixing enthalpies (per formula unit) of pseudobinary (a) $Ni_{1-x}Va_xAl$ and (b) $Al_{1-x}Ni_xNi$ B2 alloys as a function of composition.

4.2. Equilibrium lattice parameters

The equilibrium lattice parameters of B2 NiAl obtained from the relaxed SQSs are plotted in Fig. 4(a) together with the experimental X-ray measurements by Bradley and Taylor [3]. The equilibrium lattice parameter of the stoichiometric B2 NiAl is obtained in the present study to be 2.89 Å. There are four branches in Fig. 4(a), each corresponding to one of the four possible types of constitutional point defects. For the two stable branches, the present SQS calculations are in good agreement with experimental data.

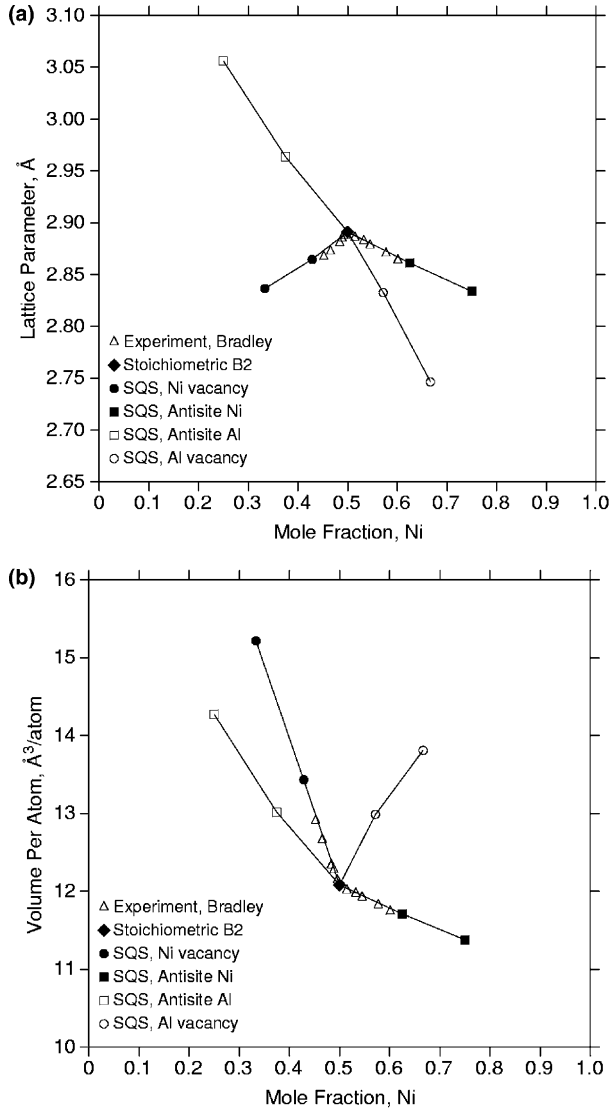

Fig. 4. Comparison between first-principles calculated and experimentally observed (a) equilibrium lattice parameter and (b) equilibrium volume per atom of B2 NiAl. Experimental data are from Bradley and Taylor [3].

In Fig. 4(b), we plot the volume per atom of B2 NiAl as a function of composition. We now observe that constitutional vacancies always increase the system volume and as the consequence, increasing pressure will suppress the formation of constitutional vacancies. On the Ni-rich side, increasing pressure will only further increase the stability of Ni antisites. Whereas on the Al-rich side, at certain crossover pressure, Ni vacancies will become unstable with respect to Al antisites, i.e., a reversal of stable constitutional point defects will occur [7,10].

4.3. Convergence tests

In this section, we further investigate if our SQSs are indeed good approximations of the random pseudobinary B2 alloys. As already mentioned, describing random alloys by periodic structures such as SQSs will surely introduce erroneous correlations beyond a certain distance. Nevertheless, as the size of the SQSs becomes larger, such periodicity error diminishes, as clearly shown in Table 3. In other words, with increasing size, the SQSs become increasingly better approximations of the real random alloys.

Table 4 shows the effects of SQS supercell size N on the calculated lattice parameters and formation enthalpies of non-stoichiometric B2 NiAl alloys. For all four alloys considered, we observed a rapid convergence of the SQSs calculated alloy properties with respect to N. Remarkably, our 8-atom SQS-4 structures already give identical lattice parameters as those given by 32-atom SQS-16 structures. For formation enthalpies, our SQS-4 structures give within 1.4 kJ/mol the results obtained using SQS-16 structures, even when local atomic relaxations are taken into account. This thus strongly indicates that those alloy properties that we considered are indeed dominated by the interactions between near neighbors. In such a case, relatively small SQSs are already sufficient to provide reliable results. Similar rapid

Table 4
Effects of SQS supercell size on lattice parameters a (Å) and formation enthalpies ΔH (kJ/mol)

Alloy	SQS-4			SQS-16		
	a	ΔH_{ur}	ΔH_r	a	ΔH_{ur}	ΔH_r
$Ni_{0.5}Va_{0.5}Al$	2.836	−41.7	−42.8	2.836	−40.3	−41.9
$Al_{0.5}Ni_{0.5}Ni$	2.834	−32.9	−33.9	2.834	−32.5	−33.1
$Al_{0.5}Va_{0.5}Ni$	2.746	−3.6	−7.9	2.746	−2.5	−9.1
$Ni_{0.5}Al_{0.5}Al$	3.056	−10.7	−18.2	3.056	−10.9	−19.5

ΔH_{ur} and ΔH_r denote unrelaxed (volume relaxations only) and fully relaxed (volume + local atomic relaxations) formation enthalpies, respectively.

convergence behavior of the SQSs has also been observed by Zunger et al. [16,17] and in our previous studies [24], which further underlines the validity of the SQS approach.

4.4. Elastic constants

Fig. 5 shows our calculated distortion energies ΔE as a function of δ^2 for various B2 NiAl alloys. The slopes of the curves at $\delta^2 = 0$ correspond to C'. For a truly harmonic crystal, the distortion energies should all fall on a straight line. Fig. 6 shows our calculated elastic bulk modulus B and shear modulus C' of B2 NiAl as a function of composition in excellent agreements with the room temperature experimental measurements by Rusovic and Warlimont [41] and Davenport et al. [42]. For a cubic structure to be mechanically stable, the three cubic elastic constants, i.e., B, C' and C_{44}, must all be positive. The present calculations and experiments both show a rapid decrease of C' with increasing Ni concentration. Beyond a critical concentration of $x^*_{Ni} \sim 0.68$, C' becomes negative, i.e., B2 NiAl becomes mechanically unstable.

Interestingly, such a structural instability of B2 NiAl coincides with the occurrence of martensitic transformation in this compound at high Ni concentrations [43,44]. Experimentally, the martensitic transformation temperature of B2 NiAl increases rapidly with Ni concentration (124 K per at.% Ni [43]), which seems to be well rationalized by the rapid softening of C' with Ni concentration: low value of C' indicates weak resistance of the B2 lattice to $\{1\,1\,0\}\langle 1\,\bar{1}\,0\rangle$ shear and thus high transformation temperature.

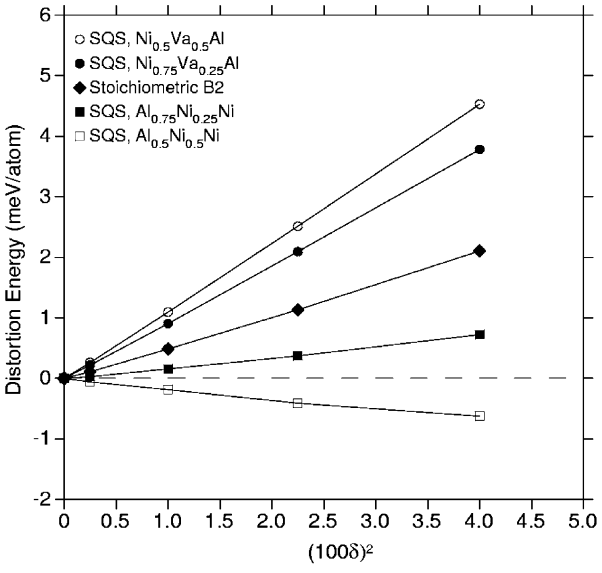

Fig. 5. Distortion energies of various B2 NiAl alloys under a homogeneous volume-conserving orthorhombic strain.

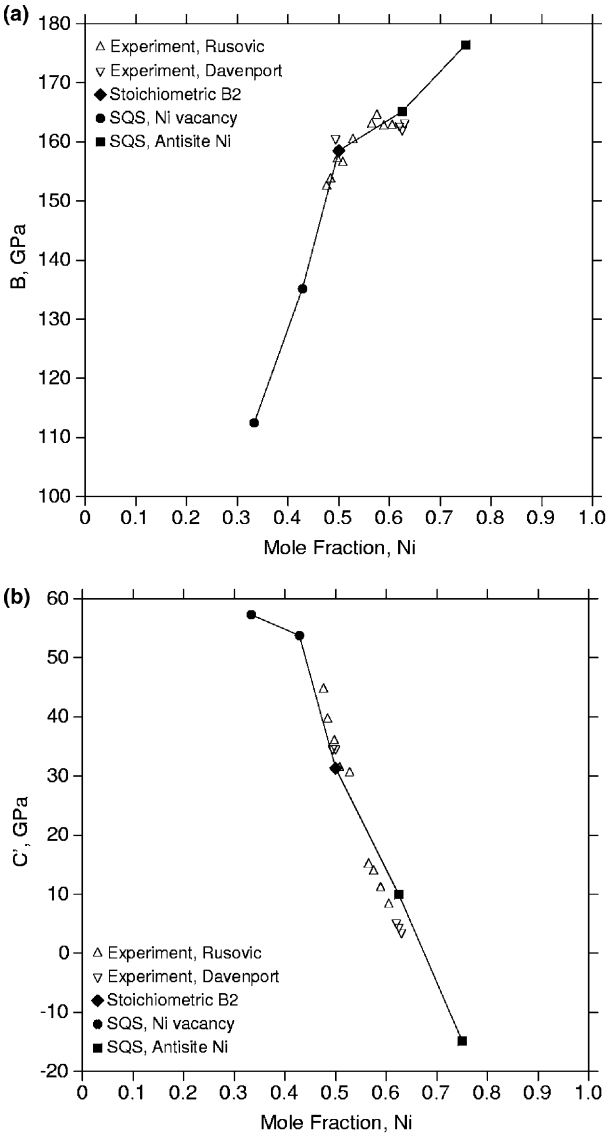

Fig. 6. Comparison between first-principles calculated and experimentally observed (a) bulk modulus B and (b) shear modulus C' of B2 NiAl. Experimental data are from Rusovic and Warlimont [41] and Davenport et al. [42].

4.5. Point defect formation enthalpies

In this section, we demonstrate how to extract formation enthalpies of isolated point defects in stoichiometric B2 NiAl from our SQS calculations at high defect concentrations. For each of the four branches in Fig. 2, we fitted our SQS calculated formation enthalpies to a quadratic function of alloy composition in the following form:

$$\Delta H(\chi) = \Delta H_{NiAl} + c_1\chi + c_2\chi^2, \tag{8}$$

where $\chi = |x_{Ni} - 0.5|$ is the absolute deviation from stoichiometry and ΔH_{NiAl} is the formation enthalpy of the perfectly ordered stoichiometric B2 NiAl. The coefficient c_1 represents the linear part of the composition depen-

Table 5
Formation enthalpies (eV/defect) of isolated point defects and complex composition-conserving thermal defects in stoichiometric B2 NiAl

Defect type	Designation	Present SQS		54-atom Supercell [13]		Experiment
		Unrelaxed	Relaxed	Unrelaxed	Relaxed	
Ni vacancy	Va_{Ni}	0.45	0.30	0.45	0.30	
Al Antisite	Al_{Ni}	2.56	1.90	2.19	1.59	
Al vacancy	Va_{Al}	1.88	1.83	1.84	1.78	
Ni Antisite	Ni_{Al}	1.09	0.99	1.12	1.04	
Triple Ni	$0 \rightarrow 2Va_{Ni} + Ni_{Al}$	1.99	1.59	2.02	1.64	1.65–1.83 [45] 1.28 [46]

Both unrelaxed (volume relaxations only) and fully relaxed (volume + local atomic relaxations) values are shown. Reference states: fcc Al and ferromagnetic fcc Ni.

dence of the alloy formation enthalpy and is directly related to the defect formation enthalpies H_d used in the Wagner–Schottky model [7,14]:

$$\Delta H = \Delta H_{\mathrm{NiAl}} + \sum_d H_d x_d, \tag{9}$$

where defect type d = Al antisite, Ni antisite, Al vacancy and Ni vacancy. x_d is the atomic concentration defined as the total number of defects of type d divided by the total number of atoms. Since $x_d = \chi$ for antisites and $x_d = 2\chi$ for vacancies, we have $H_d = c_1$ for antisites and $H_d = c_1/2$ for vacancies. The final results are given in Table 5, in good agreement with first-principles calculations using large 54-atom supercells by Jiang et al. [13]. For the purpose of comparison with experiments, we also calculated the formation enthalpy of triple-Ni defects using the formation enthalpies of isolated point defects obtained in the present study, which is in good agreement with experiments [45,46], especially when local atomic relaxations are considered.

In principle, Eq. (9) is only applicable when the defect concentrations are small. At higher defect concentrations, departure from the Wagner–Schottky model may occur due to the interactions between defects. Our SQS calculations directly considered the interactions between point defects of the same type, as indicated by the nonlinear quadratic term in Eq. (8). A direct consequence of such nonlinearity is that two branches in Fig. 2 may cross each other at certain composition and in that case a reversal of the stable constitutional point defects may occur. In fact, since simple cubic Al is energetically unfavorable with respect to bcc Al, a reversal of stable constitutional point defects from Ni vacancies to Al antisites must occur at high Al concentrations. Such a transition is, however, purely theoretical since the crossover composition is outside of the stable composition range of B2 NiAl.

5. Summary

We developed SQSs for random pseudobinary $A_{1-x}B_xC$ B2 alloys by mimicking their local pair and multisite correlation functions. The introduction of the B2 SQSs allows for the first time direct first-principles calculations of physical properties of non-stoichiometric B2 NiAl alloys containing high concentrations of constitutional point defects. The first-principles calculated lattice parameters, formation enthalpies and elastic constants are in good agreement with the experimental data in the literature. Our calculations unambiguously show that Ni vacancies and Ni antisites are the stable constitutional point defects in Al-rich and Ni-rich B2 NiAl, respectively, up to large deviations from stoichiometry. Our calculations also confirmed the experimentally observed structural instability in Ni-rich B2 NiAl, which coincides with the occurrence of martensitic transformation in this compound at high Ni concentrations. The convergence tests show that even our 8-atom SQSs are adequate to provide reliable results. We also demonstrated that our SQSs can give formation enthalpies of isolated defects in good agreement with first-principles calculations using large 54-atom supercells. Finally, the proposed B2 SQSs are quite general and can be applied to other B2 alloys.

Acknowledgments

The authors thank Dr. Axel van de Walle for providing ATAT software package. This work is funded by the National Science Foundation through Grants DMR-9983532, DMR-0122638, and DMR-0205232. The Materials Simulation Center (MSC) at Penn State led by Dr. Jorge Sofo is acknowledged for the computer resources for first-principles calculations.

References

[1] Miracle DB. Acta Mater 1993;41:649–84.
[2] Okamoto H. J Phase Equil 1993;14:257–9.
[3] Bradley AJ, Taylor A. Proc R Soc Lond A 1937;159:56.
[4] Lautenschlager EP, Kiewit DA, Brittain JO. Trans AIME 1965;233:1297.
[5] Baker I. Mater Sci Eng A 1995;193:1–13.
[6] Mishin Y, Lozovoi AY, Alavi A. Phys Rev B 2003;67:014201.
[7] Korzhavyi PA, Ruban AV, Lozovoi AY, Vekilov YK, Abrikosov IA, Johansson B. Phys Rev B 2000;61:6003–18.
[8] Fu CL, Ye YY, Yoo MH, Ho KM. Phys Rev B 1993;48:6712.

[9] Meyer B, Fahnle M. Phys Rev B 1999;59:6072.
[10] Alavi A, Lozovoi AY, Finnis MW. Phys Rev Lett 1999;83:979.
[11] Fu CL, Zou J. Acta Mater 1996;44:1471–8.
[12] Fu CL. Phys Rev B 1995;52:3151.
[13] Jiang C, Besser MF, Sordelet DJ, Gleeson B. Acta Mater 2005; 53:2101–9.
[14] Wagner C, Schottky W. Z Physik Chem B 1930;11:163.
[15] Kohn W, Sham L. Phys Rev A 1965;140:1133.
[16] Zunger A, Wei SH, Ferreira LG, Bernard JE. Phys Rev Lett 1990;65:353–6.
[17] Wei SH, Ferreira LG, Bernard JE, Zunger A. Phys Rev B 1990;42:9622–49.
[18] Hass KC, Davis LC, Zunger A. Phys Rev B 1990;42:3757–60.
[19] Lu ZW, Wei SH, Zunger A. Phys Rev B 1991;44:3387–90.
[20] Lu ZW, Wei SH, Zunger A. Phys Rev B 1992;45:10314–30.
[21] Ruban AV, Simak SI, Shallcross S, Skriver HL. Phys Rev B 2003;67:214302.
[22] Ozolins V, Wolverton C, Zunger A. Phys Rev B 1998;57:6427–43.
[23] Wolverton C. Acta Mater 2001;49:3129–42.
[24] Jiang C, Wolverton C, Sofo J, Chen LQ, Liu ZK. Phys Rev B 2004;69:214202.
[25] Lechermann F, Fahnle M. Phys Rev B 2001;63:012104.
[26] Pike LM, Chang YA, Liu CT. Acta Mater 1997;45:3709–19.
[27] van de Walle A, Asta M, Ceder G. CALPHAD 2003;26:539–53.
[28] Stokes HT, Hatch DM, FINDSYM; 2001. Available from: www.physics.byu.edu/~stokesh/isotropy.html.
[29] Blöchl PE. Phys Rev B 1994;50:17953.
[30] Kresse G, Joubert J. Phys Rev B 1999;59:1758.
[31] Kresse G, Furthmuller J. Phys Rev B 1996;54:11169–86.
[32] Kresse G, Furthmuller J. Comput Mater Sci 1996;6:15–50.
[33] Perdew JP, Wang Y. Phys Rev B 1992;45:13244–9.
[34] Perdew JP, Chevary JA, Vosko SH, Jackson KA, Pederson MR, Singh DJ, Fiolhais C. Phys Rev B 1992;46:6671–87.
[35] Monkhorst HJ, Pack JD. Phys Rev B 1972;13:5188.
[36] Kulikov NI, Postnikov AV, Borstel G, Braun J. Phys Rev B 1999;59:6824–33.
[37] Mehl MJ, Osburn JE, Papaconstantopoulos DA, Klein BM. Phys Rev B 1990;41:10311–23.
[38] Birch F. J Geophys Res 1978;83:1257.
[39] Lu ZW, Klein BM. Phys Rev Lett 1997;79:1361–4.
[40] Nash P, Kleppa O. J Alloys Comp 2001;321:228–31.
[41] Rusovic N, Warlimont H. Phys Stat Sol 1977;44:609.
[42] Davenport T, Zhou L, Trivisonno J. Phys Rev B 1999;59:3421–6.
[43] Smialek JL, Hehemann RF. Metall Trans 1973;4:1571–5.
[44] Zhang Y, Haynes JA, Pint BA, Wright IG, Lee WY. Surf Coat Technol 2003;163–164:19–24.
[45] Bai B, Collins GS. In: George EP, Yamaguchi M, Mills MJ, editors. High-temperature ordered intermetallic alloys VIII. MRS symposia proceedings, vol. 552. Pittsburgh: Materials Research Society; 1999. p. KK8.7.1-6.
[46] McCarty KF, Nobel JA, Bartelt NC. Nature 2001;412:622–5.